ECS Transactions, 58 (42) 11-17 (2014)
10.1149/05842.0011ecst ©The Electrochemical Society

Electrophoretic Deposition of Quantum Dots for Photovoltaic Applications

Seung Whan Lee*[a,b], Htay Hlaing*[a,c], Ioannis Kymissis[a,c], and Irving P. Herman[a,b]

[a] Energy Frontier Research Center, Columbia University, New York, NY 100127 USA
[b] Department of Applied Physics and Applied Mathematics, Columbia University, New York, NY 100127 USA
[c] Department of Electrical Engineering, Columbia University, New York, NY 100127 USA
*Authors contributed equally

The electrophoretic deposition (EPD) of quantum dots (QDs) after ligand exchange is investigated, along with its use as one step in the formation of photovoltaic (PV) device structures. The ligands on CdSe QDs are exchanged to pyridine and these QDs are deposited by EPD in heterojunction PV structures, which are then tested.

Introduction

Colloidal semiconductor quantum dots (QDs) are promising materials in next-generation optoelectronic devices, such as light emitting diodes, photodetectors, and solar cells due to the tunability of their bandgaps, high luminescence efficiency, narrow spectral emission, and high photostability. In particular, the push to develop third-generation solar cells that exceed the Shockley−Queisser efficiency limit for a single absorber, 31%, is one of the most fascinating challenges in the energy research field (1). In this aspect, these QDs, also known as colloidal nanocrystals, are extremely attractive because of their size-dependent properties (2), and have been used in several studies of photovoltaic devices (PVs) (3,4). However, in most cases these are films of as-synthesized QDs that have poor electrical conductivity because their surfaces are capped by insulating organic molecules, as a result of the synthesis procedure; these QDs should undergo ligand exchange before they can be used for photovoltaic applications (5).

Currently, QD-based films used in devices are often deposited by one-step spin-coating or drop-casting, sometimes as mixtures of QDs with conducting polymers (3,4). Ligand exchange of QDs is being developed using solution processing for subsequent deposition. Notably, for PV devices, post-ligand exchange has also been conducted during the layer-by-layer (LBL) deposition of QDs that is used to achieve the desired thickness (6). This type of ligand exchange to shorter and more conductive surfactant molecules involves up to three steps to deposit each very thin QD layer; many (5-20) repeated layers are needed in PV applications, and this is considered to be incompatible with mass production. Also, such ligand exchange has been limited to ligands such as ethanedithiol (5). Moreover, the choice of the final ligand is often made based on the solvent compatibility with underlying films and not the conductivity of the ligand itself.

In this study, we investigate an alternative method of forming QD films for PV and other devices: the use of electrophoretic deposition (EPD) after ligand exchange of the QDs with the goal of improving film electrical conductivity and device performance. EPD is a potential single-step solution-based route for rapid production of large-area uniform QD thin films with desired thickness. Since our initial reports on the EPD of CdSe QDs (7,8), several groups have made efforts to employ EPD in fabricating solar cells (9-12). However, the ligands in these films had the insulating TOP/TOPO/phosphonate ligands, which prevented the realization of the full potential of QDs-based solar cells. We also note that, more generally, most studies of the EPD of QD films have employed as-synthesized QDs without ligand exchange. Here, we investigate the EPD of CdSe QDs that had undergone ligand exchange in solution phase, to ligands that may improve film conductivity, prior to deposition. Specifically, we exchanged the capping ligands of CdSe QDs to pyridine, a short molecule, as a model system, and investigated the EPD of films containing these pyridine-capped CdSe QDs using a variety of solvents to form colloids for EPD. We then used this EPD process as one step in fabricating organic/inorganic hybrid, heterojunction solar cells. These devices exhibit power conversion efficiencies (PCEs) up to 0.5%.

Experimental Procedure and Results

CdSe QDs (or nanocrystals NCs) can be prepared with high quality by solution processing; they and their ligand chemistry have been intensively studied. The exchange of the initial ligand in CdSe QDs with pyridine demonstrates one successful ligand exchange (6). In our study, we exchanged the ligands on CdSe QDs from TOP/TOPO/phosphonate to pyridine, as reported earlier (6). The ligand exchange was confirmed by Fourier transform infrared spectroscopy (FT-IR), photoluminescence (PL), UV-absorbance, and energy dispersive analysis (EDS) (5). The solubility of these pyridine-capped CdSe QDs was tested in several solvents: toluene, chloroform, pyridine and isopropanol, by first precipitating the QDs in hexane and then centrifuging them. Afterwards, solvent was added and the solution was sonicated for 5 min. Figure 1a shows that pyridine-capped CdSe QDs were well dispersed in the long term only in the pyridine and chloroform solvents. Figure 1b shows the TEM of dry cast films using these four colloid solutions, right after solution preparation, which shows clustering of the QDs with toluene and isopropanol.

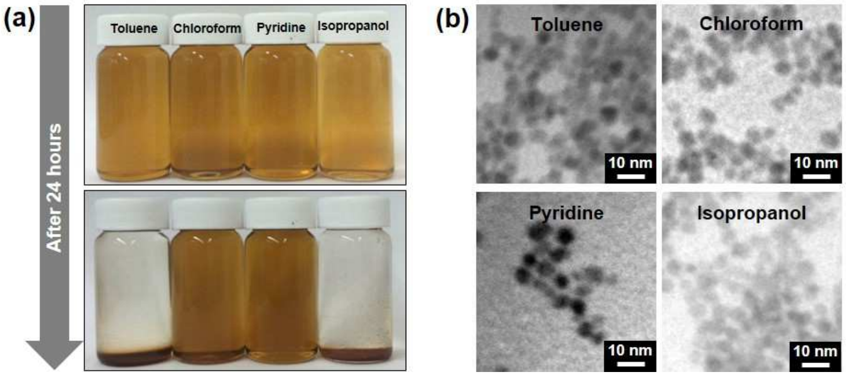

Figure 1. (a) Short- and long-term solubility of 6.0 nm diameter pyridine-capped CdSe QDs in toluene, chloroform, pyridine, and isopropanol solvents. (b) TEM images of these QDs after drop-casting these colloids right after preparation and 5 min of sonicating the QD/solvent solution

EPD of the pyridine-capped CdSe QDs in chloroform and pyridine was first tested by applying 300 V across electrodes separated by 2.3 mm by using a colloid loaded with 0.14 mg/mL of QDs. This is schematically portrayed below in Figure 4b. In these experiments, the electrodes were two 1 cm x 2.5 cm Si substrates, each overcoated by 10 nm Cr/50 nm Au by using thermal evaporation. EPD film thicknesses were measured by profilometry.

Films of these CdSe QDs were deposited by using EPD methods reported earlier (7,8). Interestingly, whereas EPD forms films of TOP/TOPO/phosphonate-capped CdSe QDs on both electrodes (7), these films formed only on the negative Au electrode, as is seen in Figure 2a, which suggests that pyridine-capped CdSe QDs are only positively charged. (This also occurred in the fabrication of PV devices, as is depicted in Figure 4b.) Electrophoretic mobility measurements presented in Figure 3 show that the QDs are positively charged in both solvents, so this is not surprising. Figure 2b shows the increase of EPD film thickness vs. time when using chloroform and pyridine solvents. The film thickness saturates at ~1500 nm in both cases. The faster initial EPD rate in chloroform than pyridine is consistent with the larger electrophoretic mobility of CdSe QDs in chloroform (13), suggested by the zeta potential measurements in Figure 3.

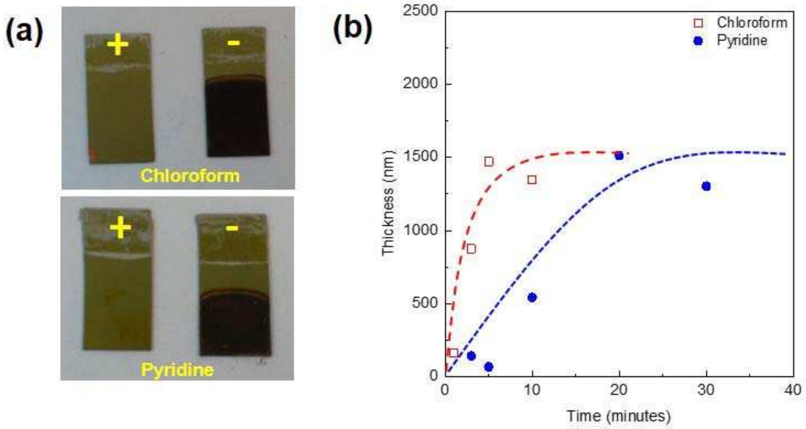

Figure 2. EPD of 6.0 nm CdSe QDs (concentration of 0.14 mg/mL, 30 mL) with 300 V applied, with (a) photographs after 30 min EPD on the positive and negative electrodes with chloroform or pyridine solvent, showing EPD only on the negative electrode, and (b) the EPD film thickness on the negative electrode vs. time.

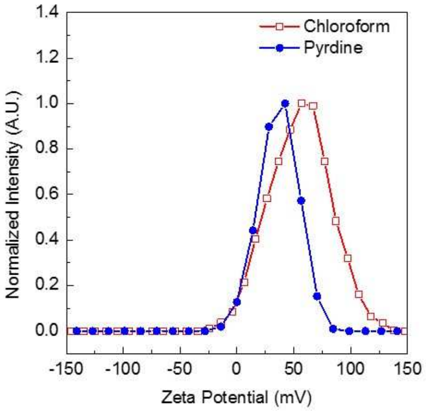

Figure 3. Zeta potential of pyridine-capped CdSe QDs (6.0 nm) in chloroform and pyridine. The electrophoretic mobility is proportional to the zeta potential.

To test PV performance, we used this EPD process as one step in forming heterojunction PV test structures, which is illustrated in Figure 4. This process started with an indium tin oxide (ITO) coated glass substrate (2 cm x 2 cm), where the transparent conductor ITO (5-15 ohms per square) had been prepatterned as a 0.4 cm-wide hexagon. (See Figure 5.) These substrates were cleaned by several steps in an ultrasonic bath: in soap water (15 min), DI water (15 min), acetone (15 min) and isopropanol (15 min), and were subsequently treated with UV-ozone for 20 min. A zinc oxide film was formed on the cleaned ITO substrate by spin-coating a solution of diethyl zinc solution in THF and subsequent hydrolysis at 150^{o}C for 15 min (14). The spin-cast ZnO thin film is insoluble in organic solvents and is used as an electron-transporting layer in solar cells. Then a film of pyridine-capped CdSe QDs was deposited on the ZnO layer (as the negative electrode) by EPD, as above, using Cr/Au on Si as the counter, positive electrode. Then, a p-type copper phthalocyanine (CuPc) organic layer, MoO_x hole-transport layer and Au electrode layer were successively deposited by thermal evaporation to complete the device stack. The targeted film thicknesses of the ZnO (60 nm), CuPc (40 nm), MoO_x (10 nm), and Au (80 nm) layers were the same in each run. They were selected using guidance from the studies of Ref. 6. The resulting devices had an active area of 0.16 cm^2. Their current density-voltage (J-V) characteristics were measured with a Keithley 2400 digital source meter under dark conditions and under AM 1.5G irradiation of 100 mW/cm^2 from a solar simulator.

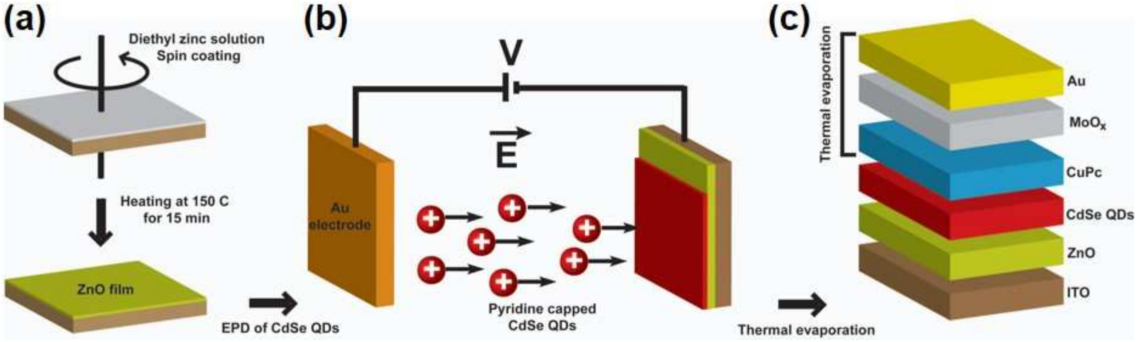

Figure 4. Fabrication of the PV device structures: (a) Forming the ZnO film on the ITO/glass substrate. (b) Schematic of the EPD process, showing pyridine-capped CdSe QD EPD occurs on only the negative electrode. (c) The layer structure of the PV device.

Device structures were first made by the method illustrated in Figure 4 with the deposition of 60 nm thick CdSe QD EPD films, using chloroform and pyridine solvents, and are depicted in Figure 5. These film thicknesses were targeted using EPD calibration curves presented in Figure 6, which is similar to Figure 2b except more measurements were made for short EPD times to enable calibrated deposition of relatively thin films. The J-V curves for these devices are shown in Figures 7a and b for dark and solar simulation conditions. The power conversion efficiency is higher using the pyridine solvent. Using EPD with pyridine solvent, the PCE was improved by varying the EPD layer thickness, which for 20 nm thickness produced a PCE of 0.53% (Figure 7c).

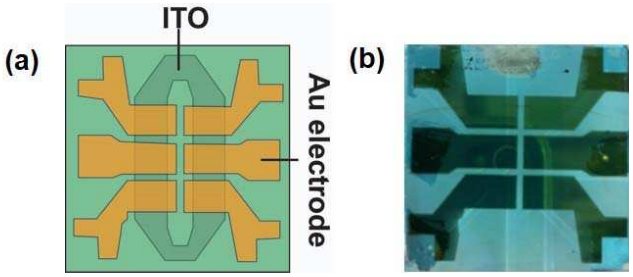

Figure 5. (a) Schematic and (b) optical micrograph of the PV structures tested in Figure 7. The overlap regions of the Au and ITO (on glass) show the active areas of six PV devices, each with dimensions 0.4 cm × 0.4 cm.

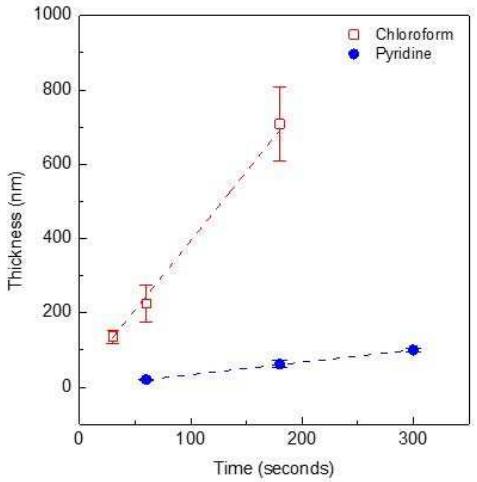

Figure 6. Calibration of EPD film thickness (5.7 nm CdSe QDs) for preparing the EPD films for the PV structures shown in Figures 4 and 5 and tested in devices in Figure 7.

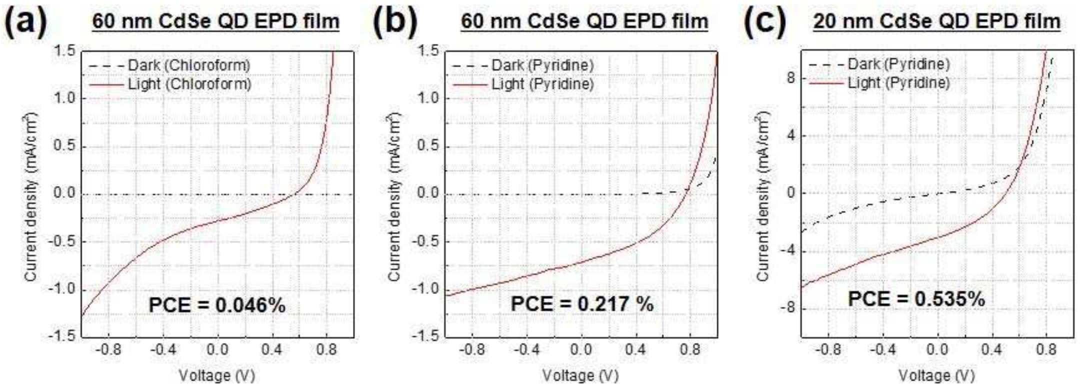

Figure 7. J-V characteristics of photovoltaic devices under dark conditions and under AM 1.5G irradiation of 100 mW/cm^2 from a solar simulator. The CdSe QDs were ~5.7 nm in diameter. The EPD film thickness was 60 nm in (a) and (b) and 20 nm in (c). The colloid solvents were chloroform in (a) and pyridine in (b) and (c).

Discussion and Conclusions

We have investigated the EPD of CdSe QDs after they had undergone ligand exchange to pyridine. The QD film thickness can be controlled by setting the EPD voltage and duration and the colloid concentration. The EPD process has the advantages of being solution-based to enable rapid fabrication and a one-step process, both potentially importance for fabricating PV devices.

Specifically, we employed EPD-deposited CdSe QD thin films as the n-type layer in organic-inorganic hybrid solar cell in conjunction with a CuPc p-type layer. It has been shown that devices of this type structure operate as excitonic solar cells with photogenerated excitons dissociating at the organic/inorganic heterojunctions (15,16). ZnO, an n-type semiconductor with relatively high electron mobility, is inserted between the ITO electrode and the active layer to effectively block holes but efficiently transport electrons to the ITO electrode. MoO_x, a well-known material with work function close to -5.3 eV, is deposited prior to the deposition of Au electrodes to efficiently extract holes.

The PV structures fabricated here have PCEs comparable with other heterojunction PVs made with CdSe QDs, as seen in Table I (5,6). However, the observed PCE is still low compared to those made other methods (17,18), likely because of non-optimized light absorption, electron and hole transport, and exciton recombination, all which need to be optimized.

TABLE I. Comparison of PV Device Structures with CdSe QDs, and ITO and Au Electrodes.

Preparation Method	Ligand	Structure	PCE
Ref. 6	ethanedithiol	ITO/CdSe/CuPc/Au	0.3%
Ref. 5	pyridine	ITO/PEDOT:PSS/CdSe:P3HT/Al	0.3%
Current work	pyridine	ITO/ZnO/CdSe/CuPc/MoO_x/Au	0.5%

We expect the results of this model EPD system can be extended to a range of QD cores and ligands, and to the fabrication of QD-based devices other than the organic-inorganic hybrid solar cell architecture chosen in this work to demonstrate the applications of EPD. Other designs of solar cells, based on the diverse set of colloidal quantum dots such as CdTe, PbS and PbSe---and CdSe, could be implemented to take advantage of the features of EPD to match device absorption with the solar spectrum better (17-19), which would improve light absorption.

Acknowledgments

This study is supported by the Energy Frontier Research Center under Award Number DE-SC0001085 with additional support by the New York State Office of Science, Technology, and Academic Research (NYSTAR) and New York State Energy Research Development Authority (NYSERDA). The authors would like to thank William Deng, Sloka Gundala, and Derek Huang for experimental assistance in phases of this work.

References

1. W. Shockley and H. J. Queisser, *J. Appl. Phys.*, **32**, 510 (1961).
2. W. W. Yu, L. Qu, W. Guo, and X. Peng, *Chem. Mater.*, **15**, 2854 (2003).
3. G. I. Koleilat, L. Levina, H. Shukla, S. H. Myrskog, S. Hinds, A. G. Pattantyus-Abraham and E. H. Sargent, " *ACS Nano*, **2**, 833 (2008).
4. B. R. Saunders and M. L. Turner, *Adv. Colloid Interface Sci.,* **138**, 1 (2008).
5. I. Lokteva, N. Radychev, F. Witt, H. Borchert, J. Parisi, and J. Kolny-Olesiak, *J. Phys. Chem. C*, **114**, 12784 (2010).
6. S. K. Saha, A. Guchhait, and A. J. Pal, *J. Appl. Phys.,* **112**, 044507 (2012).
7. M. Islam and I. P. Herman, *Appl. Phys. Lett.*, **80**, 3823 (2002).
8. M. A. Islam, Y. Xia, D. A. Telesca, Jr., M. L. Steigerwald, and I. P. Herman, *Chem. Mater.*, **16**, 49 (2004).
9. P. Brown and P. V. Kamat, *J. Am. Chem. Soc.*, **130**, 8890 (2008).
10. B. Farrow and P. V. Kamat, *J. Am. Chem. Soc.*, **131**, 11124 (2009).
11. N. J. Smith, K. J. Emmett, and S. J. Rosenthal, *Appl. Phys. Lett.*, **93**, 043504 (2008).
12. A. Salant, M. Shalom, and U. Banin, *ACS Nano*, **4**, 5962 (2010).
13. M. Zarbov, I. Schuster, and L. Gal-Or, *J. Mater. Sci.,* **39**, 813 (2004).
14. W. J. E. Beek, M. M. Wienk, and R. A. J. Janssen, *Adv. Mater.*, **16**, 1009 (2004).
15. J. J. Choi, Y.-F. Lim, M. B. Santiago-Berrios, M. Oh, B.-R. Hyun, L. Sun, A. C. Bartnik, A. Goedhart, G. G. Malliaras, H. D. Abruña, F. W. Wise, and T. Hanrath, *Nano Lett.*, **9**, 3749 (2009).
16. K. S. Leschkies, T. J. Beatty, M. S. Kang, D. J. Norris, and E. S. Aydil, *ACS Nano*, **3**, 3638 (2009).
17. J. Tang, K. Kemp, S. Hoogland, K. S. Jeong, H. Liu, L. Levina, M. Furukawa, X.Wang, R. Debnath, D. Cha, K.W. Chou, A. Fischer, A. Amassian, J. B. Asbury, and E. H. Sargent, *Nature Mater.* **10**, 765 (2011).
18. O. E. Semonin, J. M. Luther, S. Choi, H.-Y. Chen, J. Gao, A. J. Nozik, M. C. Beard, *Science*, **334**, 1530 (2011).
19. J. M. Luther, M. Law , M. C. B., Q. Song , M. O. Reese , R. J. Ellingson and A. J. Nozik, *Nano Lett.,* **8**, 3488, (2008).